NASA Technical Memorandum 100294

Friction and Wear of Monolithic and Fiber Reinforced Silicon-Ceramics Sliding Against IN-718 Alloy at 25 to 800 °C in Atmospheric Air at Ambient Pressure

Daniel L. Deadmore and Harold E. Sliney
Lewis Research Center
Cleveland, Ohio

February 1988

NASA

FRICTION AND WEAR OF MONOLITHIC AND FIBER REINFORCED SILICON-CERAMICS SLIDING AGAINST IN-718 ALLOY AT 25 TO 800°C IN ATMOSPHERIC AIR AT AMBIENT PRESSURE

Daniel L. Deadmore and Harold E. Sliney
National Aeronautics and Space Administration
Lewis Research Center
Cleveland, Ohio 44135

E-3942

SUMMARY

The friction and wear of monolithic and fiber reinforced Si-ceramics sliding against the nickel base alloy IN-718 at 25 to 800 °C was measured.

The monolithic materials tested were silicon carbide (SiC), fused silica (SiO_2), syalon, silicon nitride (Si_3N_4) with W and Mg additives and Si_3N_4 with Y_2O_3 additive. At 25 °C fused silica had the lowest friction while Si_3N_4 (W,Mg type) had the lowest wear (2.2×10^{-6} $mm^3/N-m$). This wear is considered to be in the moderate to low range. At 800 °C syalon had the lowest friction while Si_3N_4 (W,Mg type) and syalon the lowest wear (5×10^{-8} and 5.1×10^{-8} $mm^3/N-m$ respectively). This is considered to be very low wear. The SiC/IN-718 couple had the lowest total wear (ceramic rub block wear + alloy disk wear) at 25 °C. At 800 °C the fused silica/IN-718 couple exhibited the least total wear.

SiC fiber reiforced reaction bonded silicon nitride (RBSN) composite material with a porosity of 32 percent and a fiber content of 23 vol % had a lower coefficient of friction and wear when sliding parallel to the fiber direction than in the perpendicular at 25 °C.

The coefficient of friction for the carbon fiber reinforced borosilicate composite was 0.18 at 25 °C. This is the lowest of all the couples tested. Wear of this material was about two decades smaller than that of the monolithic fused silica. This illustrates the large improvement in tribological properties which can be achieved in ceramic materials by fiber reinforcement. The reason for this large improvement is the increased fracture toughness produced by the fibers.

At higher temperatures (550 to 800 °C) the oxidation products formed on the IN-718 alloy are transferred to the ceramic by sliding action and forms a thin, solid lubricant layer which decreases friction and wear for both the monolithic and fiber reinforced composites.

INTRODUCTION

Silicon-ceramics and other ceramic materials are currently receiving much attention for use in high temperature areas of heat engines and other energy conversion systems (ref. 1). These materials are candidates for cylinder liners, piston caps, and other uses. In some applications, sliding or rubbing

contact with themselves or other materials, such as metal alloys, can be expected.

Silicon-ceramics are here defined as monolithic or fiber reinforced materials of Si_3N_4, syalon (Si,Y,Al,O,N), SiC, and fused silica (SiO_2) glass. The addition of reinforcing fibers, such as SiC and carbon, to ceramic materials increases their fracture toughness (refs. 2 to 6) which improves the wear resistance (refs. 7 and 8) of brittle materials and decreases the coefficient of friction (ref. 9) if the porosities and grain size are comparable.

The purpose of the present investigation was to measure the friction and wear of monolithic and of SiC and carbon fiber reinforced Si-ceramics in unlubricated sliding contact with the nickel base alloy IN-718 at 25 to 800 °C in atomospheric air. A load of 6.8 kg (67 N) and a linear sliding velocity of 0.18 m/sec was used for monolithic SiC and 0.5 m/sec for the other materials. A double rub block test machine with line contact of the static Si-ceramic blocks against the circumferential surface of a rotating IN-718 disk was used. Friction and wear were recorded, and the sliding surfaces were examined by SEM (Scanning Electron Microscope) and EDX (Energy Dispersive X-rays).

EXPERIMENTAL

Measurements and Test Apparatus

A double rub block-line contact wear and friction apparatus was used for all tests. Figure 1(a) is a photograph of the loading and rub block support jig. Two rub blocks are pressed against the rotating disk by pressurizing the bellows, and the frictional torque is transmitted via the torque arm to a measuring and support system. The blocks are initially in nominal line contact with the disk. Uniform loading along this line is maintained by the pivoted, self-aligning block holders. The disk is 3.492 cm diameter and 1.28 cm thick, and the rub blocks are 2.22 cm long by 0.63 cm wide and 1.11 cm deep. The SiC fiber reinforced-RBSN (Reaction Bonded Silicon Nitride) material was only 0.2 cm wide so three pieces and several platinum shims had to be used for each block. The torque system is dead weight calibrated. A schematic diagram of the induction heating coil and sleeves used to bring the disk to the test temperature is presented in figure 1(b). The temperature of the disk surface is measured by an optical pyrometer.

All determinations are made in atmospheric air at ambient pressure with a relative humidity of 45 to 60 percent. Each rub block is loaded to 6.8 kg (67 N). The sliding velocity is 0.18 m/sec for the monolithic SiC test, but 0.5 m/sec for all the other materials. All tests were run for 60 min.

A determination involved the following: The sliding surface of the IN-718 disk is polished first with a dry felt cloth and levigated alumina then rinsed with distilled water. Next it is polished again with a water wet cloth and levigated alumina then rinsed with distilled water and rubbed with a clean felt cloth and finally rinsed with water followed by ethanol and dried. The rub blcoks are used as received with only an ethanol rinse to remove surface films. The arithmetic mean surface roughness (Ra) of both blocks and the disk was measured. After assembly of the test apparatus the linear sliding velocity

is set but the rub blocks are not loaded. The induction generator is turned on and the disk surface is heated over a 15 min period to the test temperature. Both blocks are now pressed against the revolving disk by pressurizing the bellows and the friction force is recorded over a period of 60 min. At the end of this time the blocks are unloaded, the induction generator is shut off, and after cooling to room temperature the blocks and disk are removed and the wear debris collected and stored.

After test, measurements are made on the blocks and disk for the purpose of determining the wear volumes. Traverse profilometer traces are taken at four locations on the wear track of the disk. In a similar way three traces are made of the wear scar of each rub block, one at each end and at the center of the scar. Squares are counted on the profilometer traces to get the area and then multiplied by the length to obtain the wear volume. Then the average wear volume was calculated.

Wear factor, K, was calculated from the average profilometer determined wear volumes by:

$$K = \text{Wear volume}(mm^3)/\text{load}(N)/\text{sliding distance}(m)$$

This value is the average wear factor over the test duration.

Energy dispersive x-ray (EDX) analysis was utilized to determine the chemical element distributions in starting materials and transferred elements in sliding contact areas. This analysis involves mounting the specimen in a scanning electron microscope (SEM) to which an x-ray detector and analyzer system are attached. An energy dispersive spectra qualitatively identifies the chemical elements present. This spectra is then quantified with built-in corrections for atomic number, atomic absorption, and fluoresence, (the so-called ZAF corrections) using a no-standard program. This program reduces the spectral line intensities to a numerical value representive of element content. If the spectral collection process is kept constant then a relative element content can be determined. That is, the element content of one area can be compared to that of another area on the same specimen or like specimens. These results must not be construed as being as accurate as when standards are used but give a good semi-quantitative elemental analyses. For example, the use of this method on a sample of as received IN-718 alloy gave results within 1 percent of the nominal content for each of the elements present.

One of two modes was used to collect spectra, a spot and an area. In the spot mode the specimen is stationary and a small electron beam spot is moved from feature to feature of interest. In the area mode the magnification is adjusted so as to cover an area of interest and the specimen is moved from area to area. Both the spot and area modes were used to examine the starting materials. The spot mode was used for small inclusions and the area mode at relatively low magnification to determine the average element content. The latter method was also used to determine the average elemental content of material transferred in wear regions. In all uses it is essential to maintain the SEM parameters constant and to calibrate the EDX analyzer and determine the detector efficiency before starting. The SEM operating conditions and EDX calibration must remain constant while spectra are collected from different areas of a specimen or different specimens.

For the determination of transfer elements in the wear scars and tracks the magnification was set so that the area analyzed was totally within the wear zone of the specimen with the smallest wear scar length. This was necessary so that when moving from one specimen to another, the analyzed area would always be totally within the scar. Four spectra are collected at random locations in the wear area of each rub block by lateral translation of the SEM stage. Once the spectra are collected they are reduced to an element content through the use of the no-standard program. This routine requires the input of the beam voltage, take-off-angle, tilt angle, elements list to be analyzed for, and the normalization value for the elements list. The elements list must be kept constant for the same relative analysis. The elements list was always normalized to 100 percent. For example, the element list for the scar analysis was Ni, Cr, Fe, Si, Ti, Mo, Al, and Nb. An average element content was determined from the four spectra. The no-standard program includes a background subtraction, overlap corrections, atomic number, absorption, and fluorescence (ZAF) matrix corrections. This program calculates comparison intensities for each element from first principles.

The SEM employed for EDX analysis also had a light element WDS (wavelength dispersive spectrometer) attachment. A line scan analysis using both the EDX and WDS instruments was made. This was used to analyze for the relative distribution of transfer elements in the wear scar along a line across a chosen feature. In this line mode an electron beam focused to a spot is driven across the feature in the wear scar and a record of element intensity for a chosen list of elements is recorded versus distance. The WDS spectometer is used for detection of oxygen and nitrogen and the EDX for the heavier elements.

Nickel and silicon in the collected wear debris was determined by spectrographic analysis. From these values the Ni/Si ratio was calculated.

Starting Materials

A listing of typical composition and other physical properties of the Si-ceramic starting materials are presented in table I. These results give some degree of characterization of the materials tested. This is a particularly appropriate exercise when dealing with ceramic materials. As will be seen most of the ceramics are not pure or totally dense but contain other constituents and have some degree of porosity.

Silicon nitride. - Two varieties of hot pressed Si_3N_4 were tested. The N-variety contained tungsten and magnesium and small amounts of other elements in addition to silicon and nitrogen. The XRD (X-ray Diffraction) pattern showed a minor Si_2W phase as well as beta-Si_3N_4 to be present. The C-variety contained 8 wt % Y_2O_3 and the XRD pattern revealed a $Y_{20}N_4Si_{12}O_{18}$ type phase in addition to beta-Si_3N_4. Both the (N) and (C) varieties are nearly 100 percent of theoretical density and the hardness was similar (1422±80 and 1320±102 kg/mm^2 respectively). A Knoop hardness for Si_3N_4 at 25 °C is reported in reference 10 as 1880 kg/mm^2. Machining groves are seen in the photomicrograph of the machined surface of the N-variety in figure 2. A photograph of the machined surface of the C-variety had a similar appearance so is not shown. These are the tested surfaces. The roughness of these surfaces is 0.25 to 0.38 μm (Ra).

Photomicrographs of the finely polished surface of these monolithic nitride starting materials are presented in figures 3 and 4. An examination of the polished and unetched materials reveals the void and inclusion distribution. These materials were polished with diamond grit. Spot EDX results of various inclusions are given along with area values. The area results were made at a low magnification (50X) and they represent the average element content of the matrix and many inclusions. White inclusions in the N-variety of Si_3N_4 were relatively higher in tungsten than the gray matrix. These inclusions are probably the Si_2W phase found by XRD. Both white and light gray inclusions can be visually identified in the C-variety nitride. The white are high in tungsten and the gray are high in yittrium. The light gray inclusions may be the $Y_{20}N_4Si_{12}O_{18}$ phase detected by XRD.

Syalon. - Syalon is a polycrystalline ceramic alloy based on silicon nitride. Many grades can be produced by varying the degree on substitution of aluminum and oxygen atoms for silicon and nitrogen respectively in the beta-silicon nitride lattice. Yttrium oxide is added to act as a liquid phase sintering aid.

The syalon tested was a hot pressed material 98 to 99 percent of theoretical density, and the XRD showed the only phase to be beta-Si_3N_4. Figure 2 is a photomicrograph of the machined surface and reveals less groove formation than the Si_3N_4 but more porosity. This is the tested surface, and its roughness (Ra) is 0.1 to 0.13 μm. The measured Vickers hardness was 1649±103 kg/mm^2. A typical hardness reported by the vendor for a similar material was 2000 kg/mm^2 at 25 °C. A photograph of the finely polished syalon is presented in figure 5 and shows a small amount of porosity and many white inclusions that are slightly richer in yittrium and leaner in aluminum than the voids and area results. These inclusions are the precipitated yittrium-silicate sintering aid. The EDX-no standard analysis of this polished surface gave 3.5 wt % Al, 8.5 wt % Y, and 88 wt % Si. No oxygen or nitrogen analysis was made.

Fused silica. - The fused silica starting material was homogeneous, transparent, of high purity, and has no porosity. The XRD pattern was that of a glassy substance (amorphous pattern). The measured Vickers hardness was 461±37 kg/mm^2 at 25 °C. This compares to a Knoop value of 570 kg/mm^2 at 37 °C reported in reference 11. The surface roughness (Ra) was 0.25 to 0.38 μm which is comparable to that of the nitrides. A photomicrograph of the machined surface before test is presented in figure 2 and reveals it to be pitted rather than groved as the nitrides.

Silicon carbide. - The SiC was a sintered material with the alpha crystal structure. It contained no excess silicon. It has a slightly porous microstructure and a Vickers hardness of 2418±180 kg/mm^2, the hardest of all the materials tested. A Knoop hardness value of 2400 kg/mm^2 is reported in reference 12 at 25 °C. Photomicrographs of the machined and polished-unetched surfaces are presented in reference 13. The machined test surface is not grooved like that of the Si_3N_4 materials but pitted and polished in appearance.

Fiber reinforced composites. - Two fiber reinforced Si-ceramic matrix materials were tested. One was a SiC fiber reinforced RBSN (Reaction Bonded Silicon Nitride). Its preparation and properties are discussed in detail in references 2 and 3. In brief it is a composite of eight layers of 140 μm diameter SiC fibers having a carbon core and a surface coating of carbon embedded

in a Si_3N_4 matrix. This composite was 23 vol % fibers. Its matrix porosity was 32 percent and the roughness of the test surface was 0.5 to 0.7 μm (20 to 30 μin.). This composite has an anisotropic structure so it was tested in two orientations: fibers perpendicular and parallel to the sliding surface. These orientations are shown in figure 6. The other fiber reinforced composite was composed of 50 vol % GY-70 carbon fibers in a 0/90° cross laminate structure bonded by a borosilicate glass number 7740. This material had nearly zero porosity and the tested surface roughness was the same as that of the former composite. The preparation and properties of this material are discussed in reference 4. This composite was tested in only one orientation which is given in figure 7.

IN-718 alloy. - Alloy IN-718 is a nickel based material with a nominal composition of Ni 53, Cr 18.5, Fe 18.5, Nb 5, Mo 3.1, Ti 0.9, Al 0.4, Si 0.3, Mn 0.2, and C 0.04 wt %. The Vickers hardness of this alloy at 25 °C was 517±4 kg/mm^2 at 100 g load. The surface finish (Ra) was 0.2 μm (8 μin.).

RESULTS AND DISCUSSION

Friction of Monolithic Si-Ceramics

Friction coefficients at the end of sliding are presented in table II and plotted in figure 8. In general the friction of the monolithic materials declines as the temperature increases and reaches a value in the range of 0.2 to 0.3 by 800 °C.

It has been reported for metals sliding against each other in an atmosphere containing oxygen that the friction was less than in oxygen free atmospheres (ref. 14). It was found that in the former case a thin oxide layer formed and this functioned as a solid lubricant.

It appeared that the decrease in friction of the Si-ceramics sliding against IN-718 in air is due to the formation of a lubricative oxide layer on the alloy with subsequent transfer to the ceramic during sliding. Measurements of the nickel transfer to the ceramic rub blocks, XRD analysis of the wear debris, and microscopic examinations were made to determine if this hypothesis was true.

Nickel transfer to the ceramic rub block was measured by the EDX method previously described. In order to normalize to unit silicon, which comes primarily from the Si-ceramic rub blocks, the Ni/Si ratio is calculated. Only the nickel transfer is considered, but all the other alloy elements were found to be present in the scar in the same proportion as in the alloy. This dictates no preferential element transfer. Figure 9 is a plot of the Ni/Si ratio as a function of the coefficient of friction with the test temperature printed near each point. The solid line is the result of a least squares fit of the data points excluding the outliers. It is apparent that as the nickel transfer increases, the friction decreases. Also, the nickel transfer tends to be highest at the higher temperatures.

This former analysis does not determine whether the metal elements transferred to the wear scar are oxides or metals. To answer this question several further measurements were made. First, the wear debris collected from many

determinations were analyzed by XRD. These results are tabulated in table III. This debris represents material lost from the sliding area of the couple so should be representative of what is forming during sliding. A chromite spinel (ref. 15) and NiO are commonly detected especially at higher temperatures. It is concluded that alloy metal oxides are formed. This conclusion was reinforced by information from a line scan for alloy elements and oxygen. Figure 10 shows the element distribution across an area in the wear scar which contains an irregular particle of suspected transfer material. Oxygen across this particle is high when the nickel is high. From this it is concluded that this particle is transfer material and that it is an alloy oxide. In areas adjacent to the particle much fine SiO_2 material was also detected. This material consists of wear debris particles.

Photomicrographs shown in figure 11 reveal the relative amounts of transfer material near the edge of the wear scars. At 25 °C the abundance of transferred matter appears to be lower than at 800 °C. This information correlates well with the above conclusion that the friction decreases with rising temperature due to oxide lubrication of the ceramics. This is based on the intuition that one would expect greater transfer to lead to lower friction.

It is observed that the coefficient of friction of the N and C-varieties of Si_3N_4 and syalon are similar at all test temperatures, indicating that these differences in composition produces little to no difference in sliding friction. However, the friction of fused silica at 25 °C is somewhat smaller than the nitrides, while, the SiC friction is higher at this same temperature.

As a point of reference the coefficient of friction of Si_3N_4 (N) sliding against itself at 25 °C was measured and a value of 0.48 was found. This value is similar to the friction when sliding on IN-718 at this temperature. The similarity in friction coefficients can be explained by the low formation and transfer of alloy element oxide lubricant to the ceramic at 25 °C. This substantiates the conclusion that when the amount of oxide lubricant formation is small little lubrication occurs.

For the purpose of information, a few literature values of unlubricated sliding friction of Si_3N_4 on itself at 25 °C are presented. Friction coefficients of 0.68 in dry nitrogen, 0.48 in air at 50 percent relative humidity, and 0.25 in distilled water have been reported (ref. 9) using a pin on disk tester. Values of 0.85 in dry nitrogen, 0.75 in air at 98 percent relative humidity, and 0.7 in water at a sliding velocity of 0.001 m/sec and a load of 10 N are reported in reference 16. These results show a wide diversity of values. The 0.48 value measured here is in the same range as the literature value for 50 percent relative humidity air reported in reference 9.

Wear of Monolithic Si-Ceramics

Wear factors for both the rub block and disk sliding members of the test couples are given in table II and presented graphically in figure 12 as a function of temperature. With the exception of the SiC all the ceramics have a lower wear factor at 800 °C than at 25 °C. In the case of both varieties of Si_3N_4 and syalon, the wear factors fall from the moderate to low wear range at 25 °C to the very low wear range at 800 °C. These compositions are the most wear resistant at all temperatures. The wear of the IN-718 disk is generally

larger than that of the ceramic and changes little with temperature, remaining in the moderate to low wear range.

Figure 13 compares the total wear factors at 25 and 800 °C. The total wear is the sum of the wear of the alloy disk and ceramic rub block. The total wear factors are generally clustered at the high end of the moderate to low wear range at 25 °C. At 800 °C they cluster nearly a decade lower, near the middle of this range. None of the couples fall in the very low wear range. Also, the composition of the rub blocks has little influence on total wear. This is due to the control of total wear by the relatively larger and constant wear of the disk. It is further observed that of all the monolithic ceramics tested, fused silica and SiC produced the least wear of the metal disk at all temperatures.

It is observed that the differences in composition of the N and C-varieties of Si_3N_4 and syalon do not make any significant difference in wear. The wear of these materials at 800 °C is the smallest of any of the Si-ceramics tested. In fact the wear is in the 10^{-8} $mm^3/N-m$ which is considered to be very low wear.

It was previously discussed that the sliding friction of the ceramic IN-718 alloy couples decreased with increasing temperature, and evidence suggested that the cause was due to the formation of a metal oxide glaze on the ceramic which acted as a solid lubricant film. From these results it appears logical to assume that the decrease in wear of the ceramics with increasing temperature is also due to this same transfer oxide glaze formation. If this is true then the wear factor should decrease with an increase of nickel oxide in the ceramic wear scar. To test this hypothesis the wear factors of the ceramic rub blocks were plotted in figure 14 as a function of the nickel transferred to the wear scar normalized to unit silicon. It is apparent, when all of the ceramics are looked at as a family, that the wear decreases as the nickel transfer increases. This plot also suggests that the first small amounts of transfer (Ni/Si ratios of less than 1) may have more lubricative value than larger amounts. However, this conclusion is clouded by the large scatter at Ni/Si ratios below 1.0.

Since the wear of the ceramics decreases with an increase in nickel transfer to the ceramic it appeared reasonable to examine the wear track on the IN-718 disk for silicon transfer to it from the ceramic. Figure 15 is a plot of the silicon transfer to the disk normalized to unit nickel as a function of the wear of the ceramic blocks. A ratio greater than 0.0057, which is that of the metal itself, would indicate transfer. It is evident, by examination of the results in figure 15, that some transfer of silicon to the metal occurs. Wear increases with increased silicon transfer which is the inverse effect of the nickel transfer to the ceramic. The greatest transfer occurred at the lower temperatures. This then suggests that when the amount of nickel transfer to the ceramic is low (at low temperatures) the silicon transferred to the disk is greatest and acts as an abrasive to the ceramics. This may possibly occur by embedment of hard ceramic wear debris particles, such as SiO_2, in the metal. The wear of sliding surfaces containing SiO_2 particles has been discussed in reference 13. Also, as the amount of glaze formation on the ceramic increases (at higher temperatures) it isolates the disk from the ceramic, therefore, less silicon (as SiO_2) is transferred to it so less abrasion of the ceramic block occurs.

The conclusion that metal oxide transfer to the ceramic acts as a lubricant to lower the couple friction, and wear of the ceramic appears to be reasonable. However, the wear of the metal disk is generally higher than the ceramic and independent of the temperature or composition of the ceramic. This suggests that the glaze formed on the ceramic is not generally a wear preventative for the disk. The lack of protection of the disk may be explained in part by the fact that it is not stationary and its constant rotation against the stationary rub blocks removes most of the oxide. Since the metal is oxidized and provides the glaze to lubricate the ceramics it is acting as a sacrificial material and therefore greater wear. Also, it may be due in part to the differences in hardness of the metal and the ceramics, with the harder ceramic materials wearing the softer metal. Materials of equal hardness usually wear equally. This latter statement is verified by the experimental wear data in table II at 25 °C for the Si_3N_4 (N)/Si_3N_4 (N) and IN-718/IN-718 couples. In both cases the wear of both the disk and blocks are nearly equal.

Macro-photographs of the wear scars on the monolithic ceramic rub blocks are presented in figures 16 to 19. The extent of edge chipping, degree of glaze formation, and change of the wear scar size with temperature can be judged. Fused silica rub blocks are transparent and during sliding provide a look at frictional heating which manifests itself as bright red flickering points of light. The uneven wear scar shape on the fused silica block at 25 °C is common when the wear of a material is very extensive. The relatively large extent of edge chipping on the fused silica blocks is apparent in figure 19. Edge chipping is less extensive on the nitrides. The deposit in the wear scar of the fused silica blocks at 800 °C is dark brown and has the appearance of a typical glaze commonly used on ceramics for decorative purposes.

Wear of a Si_3N_4 (N) rub block sliding against a Si_3N_4 (N) disk at 25 °C was determined for the purpose of comparison with the wear data for Si_3N_4 (N) sliding against an IN-718. The wear factor of the Si_3N_4 (N) rub block sliding on itself was about a decade larger when sliding on the IN-718 alloy disk. This suggests that even during low temperature sliding there may be some small but effective amount of transfer alloy element oxide lubrication of the ceramic. Total wear of the nitride/nitride and nitride/metal couples are similar (7.7×10^{-5} and 8.4×10^{-5} mm^3/N-m respectively). This is due to the larger wear of the metal disk in the nitride/metal couple. Generally in sliding couples of different hardness the softer material wears more than the harder material and couples of equal hardness wear equally.

As a point of reference, reported wear values for continuous, unlubricated sliding of Si_3N_4 on itself at 25 °C in air cluster in the range of 6×10^{-5} to 8×10^{-6} mm^3/N-m (refs. 9, 16, and 17). Our value of 3.4×10^{-5} mm^3/N-m falls within this range of values. Also, wear of Si_3N_4 on itself has been reported (ref. 9) to be a function of sliding velocity. Up to 0.2 m/sec the wear is 1×10^{-5} mm^3/N-m and is independent of velocity. At higher sliding velocities the wear rises rapidly reaching 6×10^{-5} mm^3/N-m at 0.8 m/sec. It has also been reported for many ceramics, including Si_3N_4, that reciprocating wear against themselves is about a decade higher than continuous sliding wear (ref. 17).

Friction and Wear Models for Monolithic Si-Ceramics Sliding on IN-718 Alloy

A brief and simple model of friction and wear of all the Si-ceramics sliding on IN-718 is presented and discussed.

These materials are grouped together as a family of similar materials, and the relationship between all the measurements and test conditions on friction and wear are treated by mathematical equations or models. After the trial of several possible simple models it was found that the friction coefficient of the ceramic/metal couple was best represented by the log to base 10 of (X), and wear of the ceramic by 10 to the power (X). Friction and wear are the dependent variables and (X) represents the independent variables. The indpendent variables are defined as the Ni/Si ratio in the wear scar (NS), Si/Ni ratio in the disk wear track (SN), test temperature (T) in °C, Ni/Si ratio in the wear debris (WD), and relative humidity (RH). A multiple linear regression program was used to analyse each model. The constants, term coefficients, correlation coefficient, and standard deviation were calculated. These equations are:

Friction of the ceramic/metal couple. -

$Mu = 0.56-0.039\log_{10}NS-0.11\log_{10}T+0.031\log_{10}WD+0.111\log_{10}SN+0.13\log_{10}RH.$
Correlation coefficient = 0.95
Standard deviation = 0.043

Wear of the ceramic. -

K = 10 to power (-5.8-0.09NS - 0.00017T + 0.0008WD + 4.86SN + 0.0034RH)
Correlation coefficient = 0.98
Standard deviation = 0.21

The range of the independent variables used are:

Ni/Si ratio in the wear scar (NS) is 0.07 to 20.5
Temperature (T) is 25 to 800 °C
Ni/Si ratio in the wear debris (WD) is 0.22 to 80
Si/Ni ratio in the wear track (SN) is 0.0055 to 0.46
Relative humidity (RH) is 45 to 60 percent

The use of these results is very limited and one is cautioned not to make any generalizations or use any values for the independent variables outside of the range given.

The most interesting and valid use of these equations is the information they provide about the effect of a change of an independent variable on the direction of change of the dependent variable. For example, an increase in the Ni/Si ratio in the wear scar (more lubricant glaze on the ceramic) or test temperature (produces more oxide) decreases the friction because they have negative term coefficients. The other independent variables have positive term coefficients so an increase in any of these will cause an increase in the friction. The relative humidity has the largest positive term value so it has the

greatest effect on the friction. In the case of the wear model the term coefficients for the Ni/Si ratio in the wear scar and the temperature are both negative, therefore, an increase in either will decrease the wear of the ceramic. An increase in any of the other independent variables will result in an increase in wear of the ceramic with the Si/Ni ratio in the wear track being the largest contributor (a large positive term coefficient) followed by the humidity term and the Ni/Si ratio in the wear debris making only a small contribution.

In both of the models for the ceramic/metal couples the humidity term coefficient is positive or an increase in humidity will cause an increase in friction and wear. Reports in references 9 and 16 for ceramic/ceramic couples indicate that an increase in humidity decreases the wear and friction. This contradiction of the humidity effect may be due to the difference in the nature of the sliding couples, that is, ceramic on metal in one case and ceramic on ceramic in the other.

Friction and Wear of Fiber Reinforced Si-Ceramics

The friction and wear of the SiC fiber reinforced/RBSN and carbon fiber reinforced borosilicate glass matrix composites are presented in table II. These materials are anisotropic in structure so friction and wear may vary with sliding direction and fiber orientation. The test direction and orientation are depicted in figures 6 and 7.

Measurements parallel and perpendicular to the fibers were made for the SiC fiber/RBSN at 25 °C. Both the wear and friction were the least when sliding was parallel to the fiber. In fact the parallel friction was about half that of the perpendicular orientation and less than any of the monolithic ceramics. The wear of the parallel sliding blocks was larger than the monolithic Si_3N_4 and SiC, but considering the large porosity and less than ideal multilayered test specimen configuration used, the composite wear is considered to be very good. With a decrease in porosity and a single piece test specimen, the fiber reinforced composite should have much lower wear. In fact the composite wear would be expected to be less than the monolithic material due to the higher fracture toughness of the composite. This conclusion is based on additional information to be discussed in subsequent paragraphs.

Figure 20 is a macro-photograph of the SiC fiber/RBSN composite specimens after test. It is clearly evident from examination of both the top and side views that the wear is less in the parallel sliding at 25 °C.

Photomicrographs of the surfaces of the SiC fiber/RBSN composite material before and after sliding are presented in figures 21 and 22. In perpendicular sliding an increased amount of edge chipping can be seen compared to parallel sliding. This edge chipping leaves a smaller specimen width to carry the load and may contribute to increased wear. The test of a one piece specimen would minimize this effect, because three specimens have six edges while one would have only two.

Some relevant but unpublished data of the authors, for a SiC whisker reinforced hot pressed Al_2O_3 sliding on IN-718 alloy in air, shows a progressive decline in wear with increasing whisker content. Likewise, the cross bending

strength and fracture toughness increases with whisker content. At 25 vol % SiC whisker content the wear is decreased by a decade at both 25 and 800 °C.

The SiC fiber/RBSN material was also tested in perpendicular sliding at 800 °C, and the decreased wear compared to the 25 °C test is dramatically illustrated in figure 20 especially in the side view. This is due to the transfer of oxide to the composite, forming a thin solid lubricant layer. This is an excellent illustration of the lubricating power of the transfer glaze. Figure 21(d) seems to suggest that the porous matrix and fiber ends may act to trap the lubricant and so enchance the supply of lubricating glaze material.

Friction test results for the carbon fiber reinforced borosilicate glass matrix composite at 25 °C, using the orientation given in figure 7, was 0.18 the lowest of any couple tested at any temperature. The wear of this composite was similar to that of the monolithic nitrides. It is interesting to note that the wear is almost two decades smaller than that of the monolithic fused silica glass. This illustrates the enchanced tribological properties provided to brittle ceramics by fiber reinforcement. The fibers increase the fracture toughness and may also provide lubrication. One of the recognized wear mechanisms of brittle materials is fracture, therefore, the increased fracture toughness provided by the fibers decreases the wear. Measurements on this carbon fiber/glass composite in air were not made at higher temperatures because of the presence of the oxidizable fibers.

CONCLUSIONS

After investigation of the unlubricated friction and wear of monolithic and fiber reinforced Si-ceramics sliding against IN-718 in air at temperatures of 25 to 800 °C the following conclusions have been made.

1. The monolithic ceramic with the lowest friction coefficient at 25 °C was fused silica, but at 800 °C it was syalon.

2. The monolithic ceramic with the lowest wear was Si_3N_4 (N) at both 25 and 800 °C. At 25 °C the wear was in the moderate to low range (10^{-5} to 10^{-6} $mm^3/N-m$), but at 800 °C it was in the very low range (10^{-7} $mm^3/N-m$ or less).

3. Monolithic SiC exhibited the lowest total wear (ceramic + metal disk) at 25 °C, but at 800 °C it was fused silica. In both couples the wear was in the moderate to low range.

4. At temperatures of 550 and 800 °C, the oxidation products of the IN-718 alloy transfer to the ceramic rub block and provide a thin, solid lubricant glaze layer which decreases friction and wear of both the monolithic and fiber reinforced composites.

5. The SiC fiber/RBSN composite sliding parallel to the fiber direction had lower wear and friction at 25 °C than sliding perpendicular to the fibers.

6. The carbon fiber/borosilicate glass composite possessed the lowest friction and total wear at 25 °C of all the couples studied at this temperature.

7. Wear of the carbon fiber/borosilicate glass composite was almost two decades lower than the monolithic fused silica glass at 25 °C. This illustrates the large improvement in tribological properties of ceramics which can be obtained by fiber reinforcement.

ACKNOWLEDGMENT

The authors thank Ramakrishna Bhatt for providing the SiC fiber reinforced/RBSN test materials.

REFERENCES

1. Kaminsky, M.; and Michaels, A.I., eds.: Tribology Project, Energy Conversion and Utilization Technologies Division, Office of Energy Systems Research, Quarterly Progress Report, Jan.-Mar. 1985, TRIB-ECUT-85-2, DOE, Apr. 1985.

2. Bhatt, R.T.: Effects of Fabrication Conditions on the Properties of SiC Fiber Reinforced Reaction-Bonded Silicon Nitride Matrix Composites. NASA TM-88814, 1986.

3. Bhatt, R.T.: Mechanical Properties of SiC Fiber-Reinforced Reaction-Bonded Si_3N_4 Composites. NASA TM-87085, 1985.

4. Minford, E.J.; and Prewo, K.M.: Wear Studies of Fiber Reinforced Glass Matrix Composites. UTRC-R83-91674-2, United Technology Research Center, Nov. 1983.

5. Prewo, K.M.; and Brennan, J.J.: High Strength Silicon Carbide Fibre-Reinforced Glass-Matrix Composites. J. Mater. Sci., vol. 15, no. 2, Feb. 1980, pp. 463-468.

6. Brennan, J.J.; and Prewo, K.M.: Silicon Carbide Fibre Reinforced Glass-Ceramic Matrix Composites Exhibiting High Strength and Toughness. J. Mater. Sci., vol. 17, no. 8, Aug. 1982, pp. 2371-2383.

7. Hornbogen, E.: Description of Wear of Materials with Isotropic and Anisotropic Microstructures. Wear of Materials, K.C. Ludema, ed., ASME, 1985, p. 477.

8. Hornbogen, E.: The Role of Fracture Toughness in the Wear of Metals. Wear, vol. 33, 1975, pp. 251-259.

9. Ishigaki, H., et al.: Friction and Wear of Hot Pressed Silicon Nitride and Other Ceramics. Wear of Materials, K.C. Ludema, ed., ASME, 1985, pp. 13-21.

10. Lankford, J.: Comparative Study of the Temperature Dependence of Hardness and Compressive Strength of Ceramics. J. Mater. Sci., vol. 18, no. 6, June 1983, pp. 1666-1674.

11. Fleming, J.D.: Fused Silica Manual, Final Report AF-40-1-2483, USAE, Eng. Expt. Station, Ga. Inst. of Techn., Sept, 1964.

12. Wu, C.C.; Rice, R.W.; and Platt, B.A.: Wear and Microstructure of SiC Ceramics. Ceram. Eng Sci. Proc., vol. 6, no. 7-8, July-Aug. 1985, pp. 1023-1039.

13. Deadmore, D.L.; and Sliney, H.E.: Friction and Wear of Sintered Alpha SiC Sliding Against IN-718 Alloy at 25 to 800°C in Atmospheric Air at Ambient Pressure. NASA TM-87353, 1986.

14. Stott, F.H.; and Wood, G.C.: The Influence of Oxides on the Friction and Wear of Alloys," Tribol. Int., vol. 11, no. 4, Aug. 1978, pp. 211-218.

15. Barrett, C.A.; Garlick, R.G.; and Lowell, C.E.: High Temperature Cyclic Oxidation Data, Vol. 1-Turbine Alloys. NASA TM-83665, 1984.

16. Fischer, T.E.; and Tomizawa, H.: Interaction of Tribochemistry and Microfracture in Friction and Wear of Silicon Nitride. Wear of Materials, K.C. Ludema, ed., ASME, 1985, pp. 22-32.

17. Cranmer, D.C.: Friction and Wear Properties of Monolithic Silicon-Based Ceramics. J. Mater. Sci.," vol. 20, no. 6, June 1985, pp. 2029-2037.

TABLE I - COMPOSITION AND PROPERTIES OF Si-CERAMIC RUB BLOCKS BEFORE TEST

Material	Typical composition,[a] wt % (unless otherwise noted)	XRD results[b]	Machined surface roughness Ra	Bulk density, g/cm3	Vickers hardness at 25°C, kg/mm2[i]
Si_3N_4 (N), hot pressed	Mg 0.4 to 0.6 Al .2 to .3 Fe .2 to .3 Ca .006 to .03 Mn .05 B < .003 W 1.5 to 2	β-Si_3N_4 (S) Si_2W (W) (card no. 11-195)[g]	10 to 15 μin (0.25 to 0.38 μm	3.20 to 3.25 ~100 percent TD[d]	1422 ±80 (100 g load)
Si_3N_4 (C), hot pressed	$8Y_2O_3$	β-Si_3N_4 (S) $Y_{20}N_4Si_{12}O_{18}$ (W) (card no. 30-1465)[g]	10 to 15 μin (0.25 to 0.38 μm)	3.25 to 3.29 ~100 percent TD	1320 ±102 (100 g load)
Syalon, hot pressed	Si,N,Al,Y,O (Si 88, Al 3.5, Y 8.5)[h]	β-Si_3N_4 (S)	4 to 5 μin (0.1 to 0.13 μm)	3.20 to 3.22 98 to 99 percent TD	1649 ±103 (200 g load)
SiO_2, transparent fused silica	B < 0.001 ppm Ca < 0.005 Cr 10 Fe 180 K < 0.01 Li < 0.1 Mg < 0.005 Na < 0.01	Broad-diffuse peaks characteristic of amorphous (glassy) materials	10 to 15 μin) (0.25 to 0.38 μm)	2.19 to 2.20 ~100 percent TD	461 ±37 (50 g load)
SiC, sintered[c]	SiC 98 B 0.6 Al 0.07 Fe 0.3 C 1	α SiC	10 to 15 μin (0.25 to 0.38 μm)	3.13 ~97.5 percent TD	2418 ±180 (200 g load)
SiC fiber reinforced reaction bonded Si_3N_4 matrix	Fibers are β SiC with pyrolitic graphite core and carbon-rich coating. Matrix is a mixture of α&β Si_3N_4, 23 vol % fibers.[e]	(-)	Perpendicular to fibers 20 to 25 μin (0.5 to 0.62 μm). Parallel to fibers 20 to 30 μin (0.5 to 0.75 μm).	2.42 (Matrix porosity, 32 percent	(-)
Carbon fiber reinforced borosilicate glass matrix	Fibers are GY70 carbon. Matrix is 7740 borosilicate glass (50 vol % fibers).[f]	(-)	20 to 30 μin (0.5 to 0.75 μm)	2.05	(-)

[a]Vendor analysis unless otherwise noted.
[b]S = Strong pattern.
W = Weak pattern.
[c]Reference 13.
[d]Percent of theoretical density.
[e]References 2 and 3.
[f]Reference 4.
[g]Card in ASTM-x-ray powder data file.
[h]By EDX analysis of polished surface.
[i]Hardness with standard deviation.

TABLE II - WEAR AND FRICTION DATA FOR Si-CERAMIC SLIDING COUPLES AT A LOAD OF 6.8 kg (67 N) AND SLIDING VELOCITY OF 0.5 m/sec (EXCEPT SiC WHICH WAS 0.18 m/sec) AND 60 min OF SLIDING

Sliding couple		Temperature, °C	Wear factor, $mm^3/N-m$		Element transfer		Ni/Si ratio in wear debris	Average coefficient of friction at 1800 m of sliding
Disk material	Rub block material		Disk	Rub block	Ni/Si ratio in disk wear track	/ Ni/Si ratio in rub block wear scar		
IN-718, alloy	αSiC	25	7.7×10^{-6}	3.1×10^{-6}	0.08	0.05	14	[b]0.62
		350	4.1×10^{-6}	3.8×10^{-6}	.076	0.4	14	.56
		550	5.8×10^{-6}	1.2×10^{-6}	.046	3.4	11.4	.34
		800	7.3×10^{-6}	8×10^{-6}	.083	0.1	6.2	.3
IN-718	Si_3N_4 (N)	25	8.2×10^{-5}	2.2×10^{-6}	.0115	1.9	51	.5
		350	1.6×10^{-4}	1.7×10^{-6}	.0132	1.3	71	.35
		550	7.6×10^{-6}	2.9×10^{-7}	.0075	10.3	48	.32
		800	1.6×10^{-5}	5×10^{-8}	.0055	20.5	68	.29
IN-718	Si_3N_4 (C)	25	8×10^{-5}	3.1×10^{-6}	.014	1.8	[a](-)	.46
		350	4.4×10^{-5}	2.4×10^{-6}	.038	.6	79	.41
		550	7.2×10^{-6}	4.6×10^{-7}	.016	8	75	.31
		800	1.4×10^{-5}	8.2×10^{-8}	.008	3.5	14	.27
IN-718	Syalon	25	6.8×10^{-5}	2.3×10^{-6}	.0097	4.3	6.4	.44
		800	1.2×10^{-5}	5.1×10^{-8}	.0097	15.3	13	.23
IN-718	Fused silica	25	9.2×10^{-6}	2×10^{-4}	.46	.07	0.22	.32
		350	5.2×10^{-6}	9.4×10^{-6}	.12	.2	(-)	.39
		550	5.3×10^{-6}	6.8×10^{-7}	.024	2.8	(-)	.32
		800	6.8×10^{-6}	1.3×10^{-6}	.017	2.4	1.1	.26
Si_3N_4 (N)	Si_3N_4 (N)	25	4.3×10^{-5}	3.4×10^{-5}	------	-------	(-)	.48
IN-718	SiC fiber - RBSN matrix (sliding perpendicular to SiC fibers)	25	4.5×10^{-4}	2.8×10^{-4}	------	-------	6.1	.37
		800	1.5×10^{-5}	3.8×10^{-7}	------	-------	6.1	.25
In-718	SiC fiber - RBSN matrix (sliding parallel to SiC fibers)	25	$1.4\ 10^{-4}$	6.2×10^{-5}	------	-------	6.0	.20
IN-718	Carbon fiber - borosilicate glass matrix	25	1.8×10^{-6}	4.2×10^{-6}	------	-------	-----	.18
IN-718	IN-718	25	4.1×10^{-5}	5.5×10^{-5}	[c].0057	[c]177	(-)	.48
		800	2.6×10^{-5}	5.2×10^{-6}	.0057	177	(-)	.31

[a]No material left after XRD.
[b]At 648 m of sliding.
[c]Calculated from metal composition.

TABLE III - XRD RESULTS OF WEAR DEBRIS FOR Si-CERAMIC/IN-718 WEAR COUPLES

Sliding wear couple		Components detected in wear debris			
Disk	Rub Block	25 °C	350 °C	550 °C	800 °C
IN-718	Fused silica	Spinel[a] (8.30)[b] (S)[c] FCC (NiSS)[d] (S)	Spinel (8.30)	Spinel (8.30)	Spinel (8.30)
IN-718	Si_3N_4 (C)	FCC (NiSS) (S)	Spinel (8.30) (S) FCC (NiSS) (S)	Spinel (8.30) (S) FCC (S)	Spinel (8.30) (S) FCC (NiSS) (S)
IN-718	Si_3N_4 (N)	FCC (NiSS) (S)	Spinel (8.30) (W) FCC (NiSS) (S)	Spinel (8.30) (S) FCC (S)	Spinel (8.30) (S)
IN-718	Syalon	FCC (NiSS) (S)	(-)	(-)	Spinel (8.30) (S)
IN-718	SiC	(-)	SiC (S) NiO (W)	SiC (S) NiO (W)	(-)
IN-718	SiC fiber - RBSN matrix (perpendicular sliding)	FCC (NiSS) (S) SiC (W) Si_3N_4 (W)	(-)	(-)	FCC (NiSS) (S) Spinel (a_0 = 8.35) (W) NiO (W)
IN-718	SiC fiber - RBSN matrix (parallel sliding)	FCC (NiSS) (S) SiC (W) Si_3N_4 (W)	(-)	(-)	(-)

[a]Chromite spinel - $((Fe^{+2}/Ni)(Fe^{+3}/Cr)_2)O_4$ (ref. 15).
[b]Lattice parameter (angstroms)
[c]S = strong pattern.
W = weak pattern.
[d]FCC (NiSS) means IN-718 alloy (face centered cubic Ni solid solution (ref. 15)).

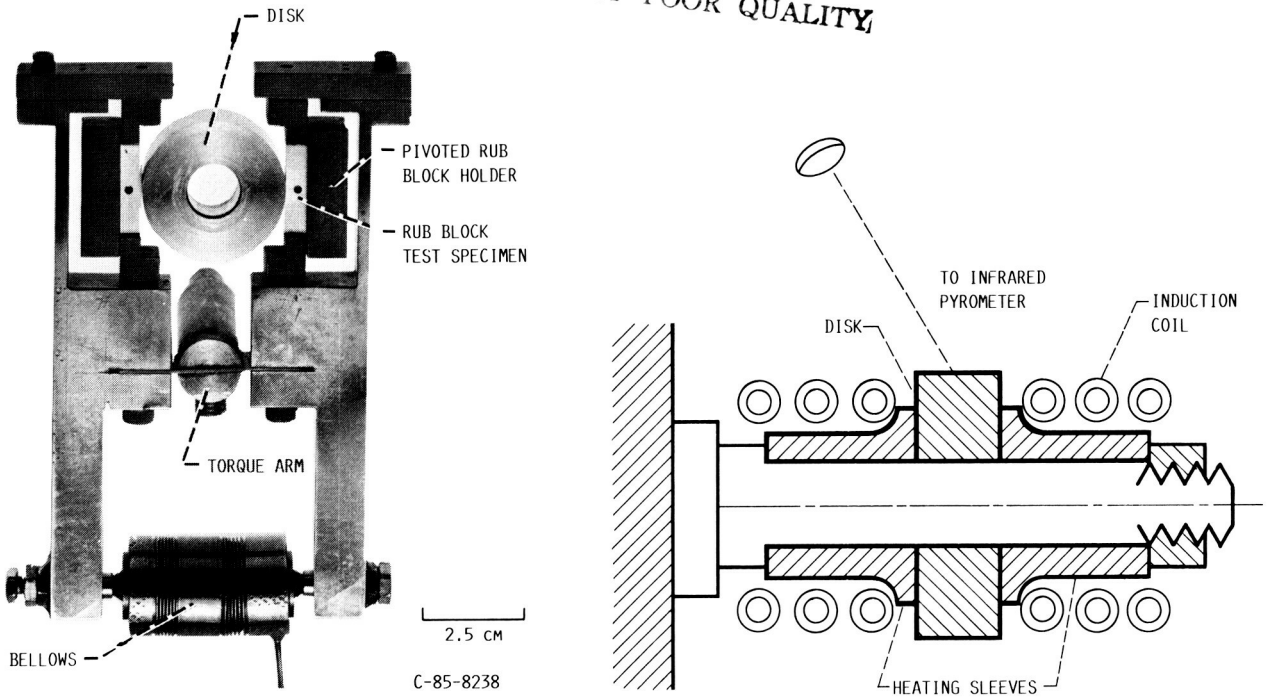

(A) PHOTOGRAPH OF LOADING AND RUB BLOCK SUPPORT.

(B) DISK HEATING SCHEMATIC.

FIGURE 1. - DOUBLE RUB BLOCK FRICTION AND WEAR TESTER.

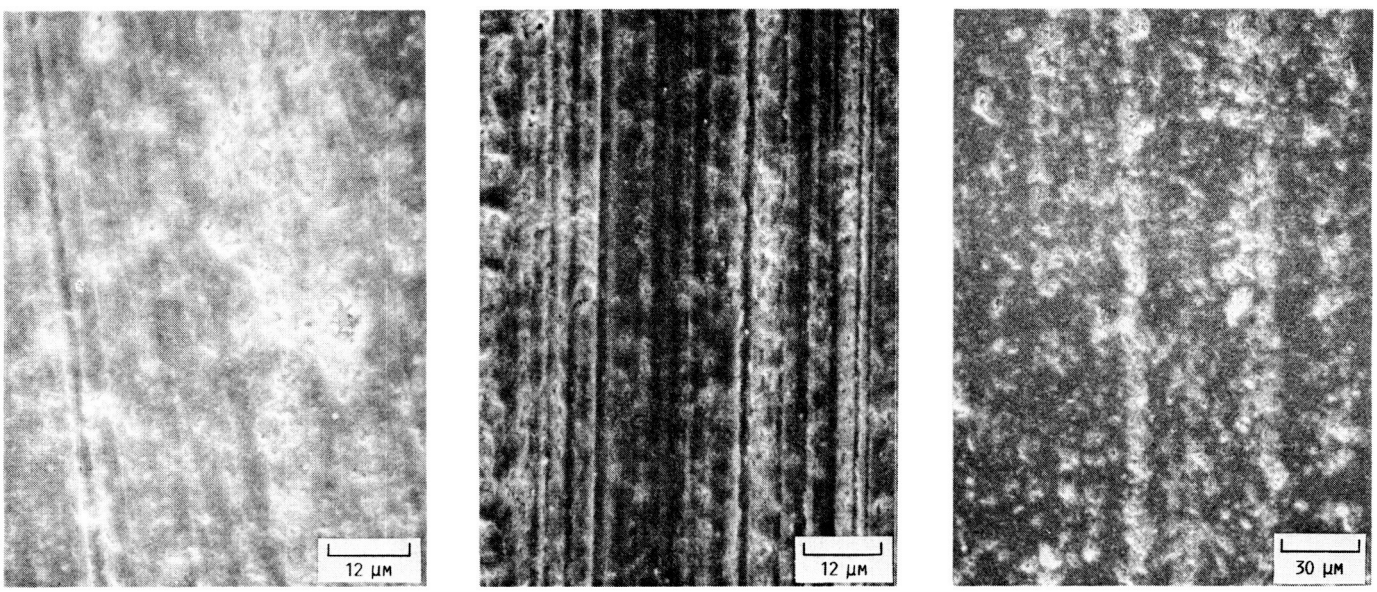

(a) SYALON.

(b) Si_3N_4(N).

(c) FUSED SILICA.

FIGURE 2. - SEM PHOTOMICROGRAPHS OF THE MACHINED SURFACE OF THE Si - CERAMIC RUB BLOCKS. (100Å GOLD COATED FOR SEM.).

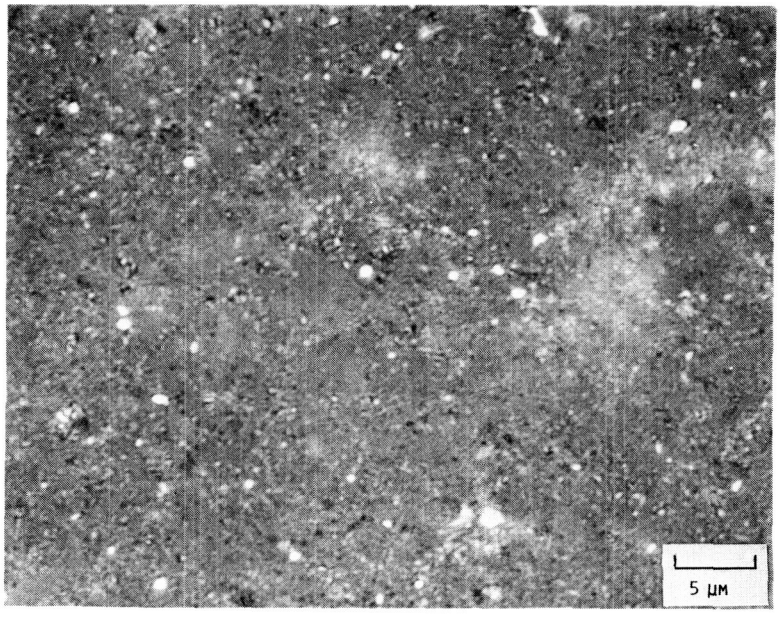

(a) PHOTOMICROGRAPH OF POLISHED AND UNETCHED SURFACE. BLACK AREAS ARE VOIDS.

	TOTAL AREA	SPOT MODE	
		WHITE INCLUSIONS	GRAY MATRIX
Mg	Q	1.4	Q
Al	0.1	1.6	0.1
Si	96.	63.	97.
Fe	0.2	Q	0.2
W	3.7	34.	2.7

(b) RESULTS OF EDX - NO STANDARD ANALYSIS.

FIGURE 3. - PHOTOMICROGRAPH AND EDX - NO STANDARD ANALYSIS OF FEATURES OF Si_3N_4(N). POLISHED AN UNETCHED SURFACE.

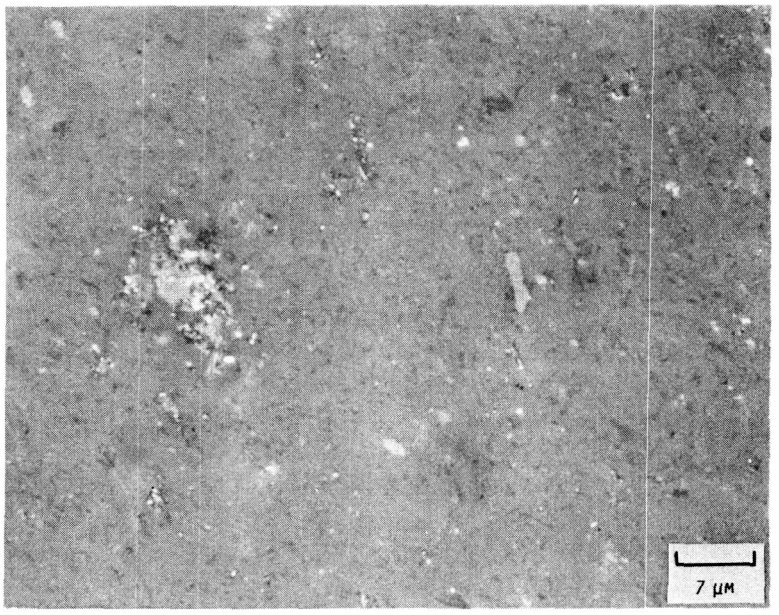

(a) PHOTOMICROGRAPH OF POLISHED AND UNETCHED SURFACE. BLACK AREAS ARE VOIDS.

		SPOT MODE		
		INCLUSION		DARKER
	TOTAL AREA	WHITE	LITE GRAY	GRAY MATRIX
Mg	0	0.7	0	0
Al	1.7	2.0	2	0.5
Si	92.8	58.5	90.8	97.2
Fe	0.1	0	0.7	0.2
Y	5.3	0	5.8	1.6
W	0.1	38.8	0.7	0.5

(b) RESULTS OF EDX - NO STANDARD ANALYSIS.

FIGURE 4. - PHOTOMICROGRAPH AND EDX - NO STANDARD ANALYSIS OF FEATURES IN Si_3N_4(C). POLISHED AND UNETCHED SURFACE.

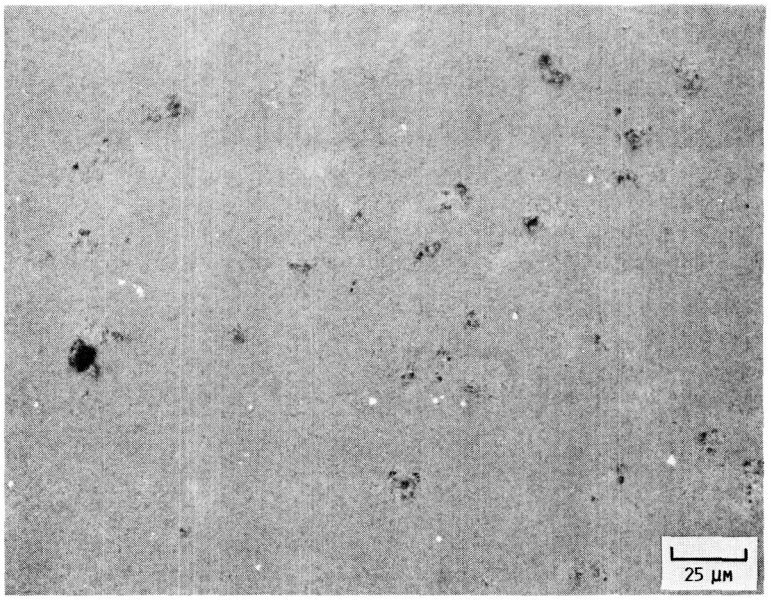

(a) PHOTOMICROGRAPH OF POLISHED AND UNETCHED SURFACE. (WHITE AREAS ARE INCLUSIONS, BLACK AREAS ARE VOIDS).

		SPOT MODE	
	TOTAL AREA	WHITE INCLUSIONS	VOID
Al	3.5	0.2	3.9
Y	8.5	10.8	8.5
Si	88	89	87.6

(b) RESULTS OF EDX - NO STANDARD ANALYSIS.

FIGURE 5. - PHOTOMICROGRAPH AND EDX - NO STANDARD ANALYSIS OF FEATURES OF SYALON. POLISHED AND UNETCHED SURFACES.

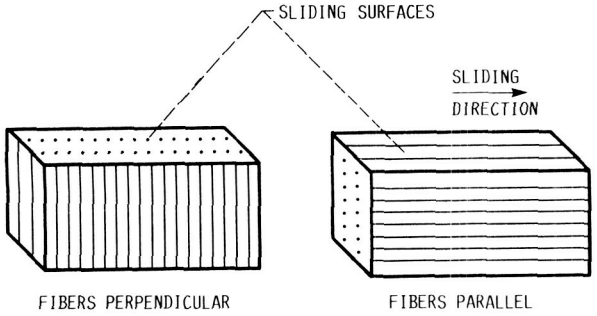

FIGURE 6. - SiC REINFORCED RBSN RUB BLOCK TEST SPECIMEN ORIENTATION ACCORDING TO FIBER DIRECTION. SLIDING DIRECTION AND SLIDING SURFACE.

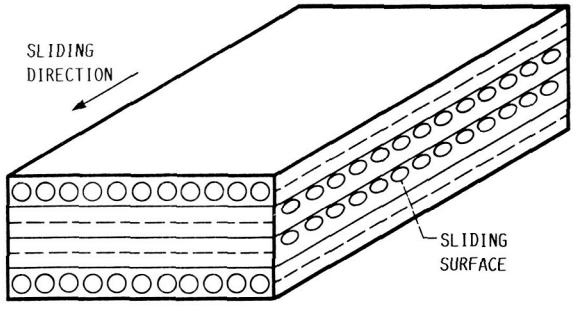

FIGURE 7. - CARBON FIBER REINFORCED BOROSILICATE GLASS MATRIX 0/90 CROSS LAMINATE RUB BLOCK TEST SPECIMEN.

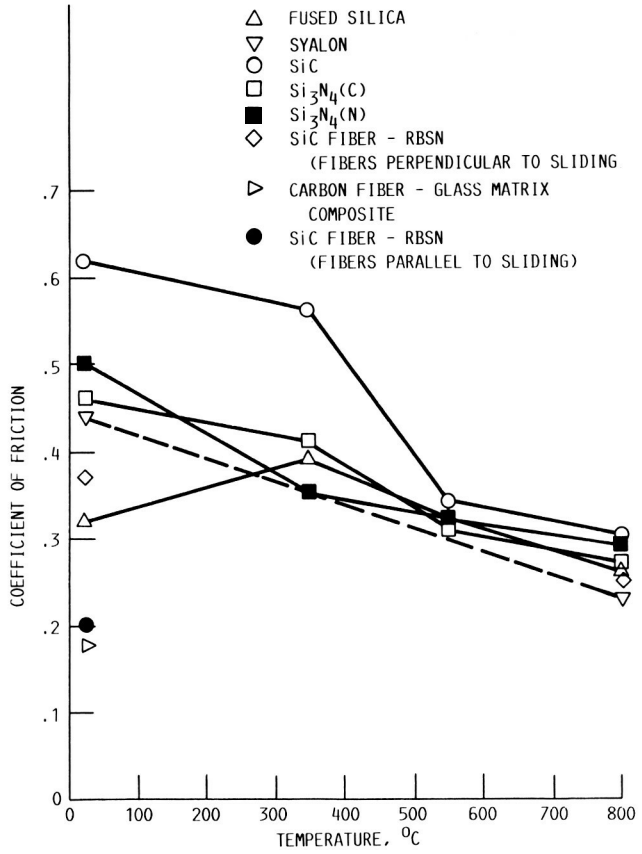

FIGURE 8. - COEFFICIENT OF FRICTION OF Si - CERAMICS SLIDING AGAINST IN-718 AT 1800 m IN AIR (AT 648 m FOR SiC) VERSUS TEMPERATURE.

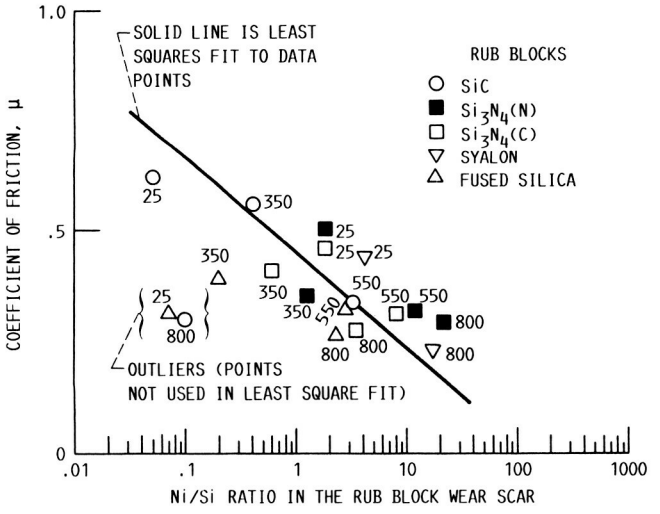

FIGURE 9. - IN718 ALLOY ELEMENT TRANSFER TO THE RUB BLOCKS VERSUS COEFFICIENT OF FRICTION (μ) AFTER SLIDING 1800 m AT 6.8 kg (67N) LOAD IN AIR (45-60% RH) AT 25-800 °C. (648 m FOR SiC) NUMBERS NEAR POINTS ARE TEST TEMPERATURE °C.

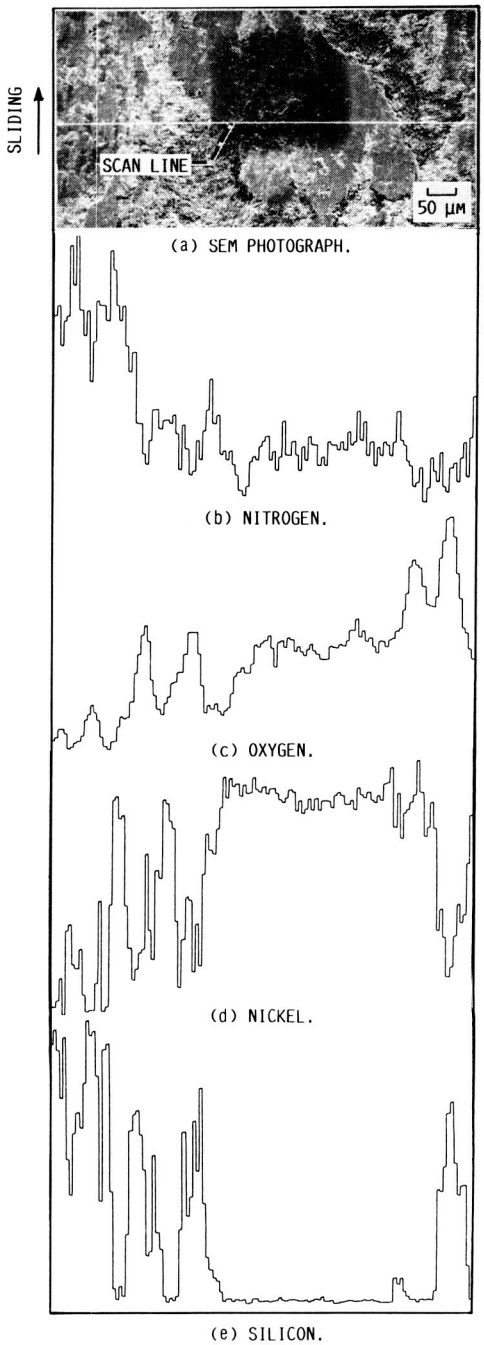

FIGURE 10. - LINE SCAN FOR O, N, Ni AND Si AND SEM PHOTOGRAPH OF WEAR SCAR ON Si_3N_4(N) AFTER SLIDING 1800 m AT 800 °C. (DARK AREA IN PHOTOGRAPH WAS CAUSED BY ELECTRON BEAM.). (GOLD COATED - 100 ANGSTROMS.)

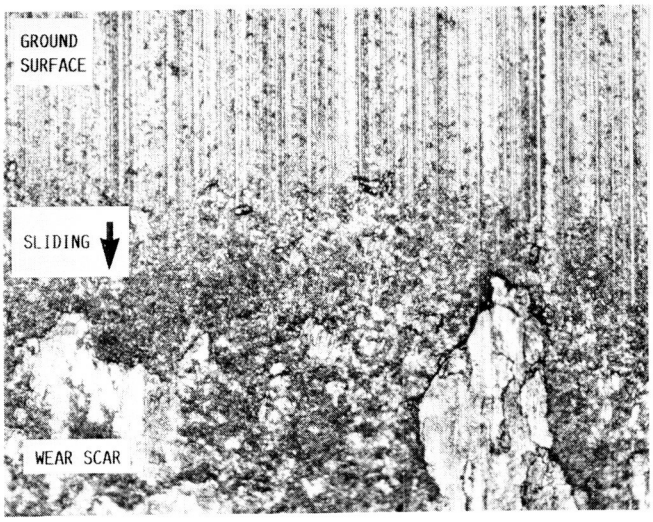

(a) Si_3N_4(N) - 25 ^{o}C.

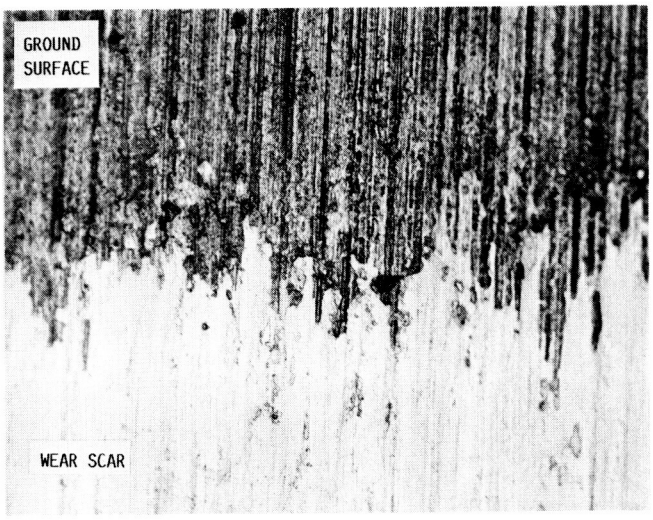

(b) Si_3N_4(N) - 800 ^{o}C.

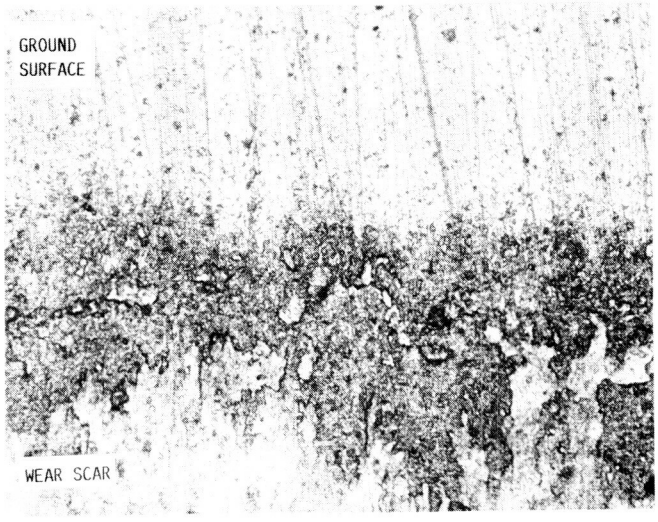

(c) SYALON - 25 ^{o}C.

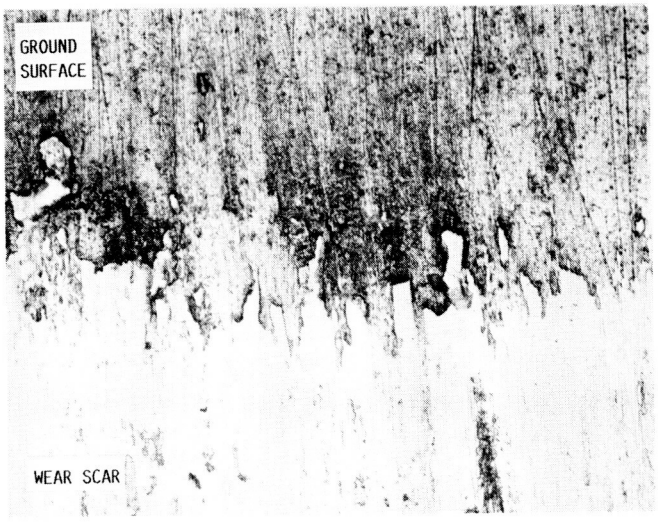

(d) SYALON - 800 ^{o}C.

(e) FUSED SILICA - 25 ^{o}C.

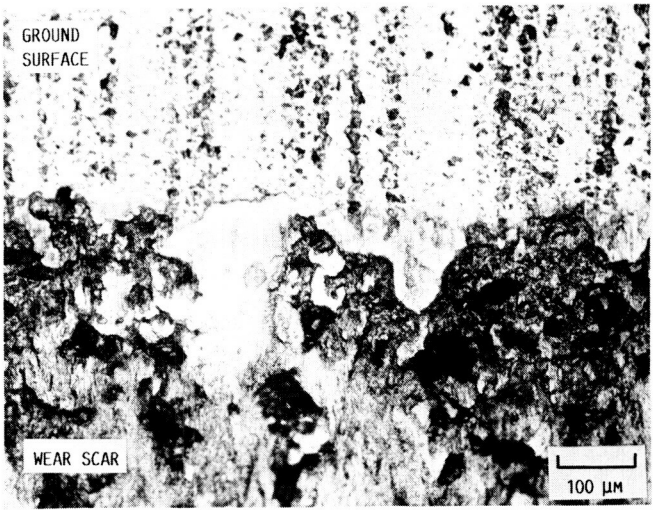

(f) FUSED SILICA - 800 ^{o}C.

FIGURE 11. - PHOTOMICROGRAPHS OF Si-CERAMIC WEAR SCARS AFTER SLIDING 1800 m AGAINST IN-718 IN AIR AT 0.5 m/sec AND A LOAD OF 6.8 kg (67N).

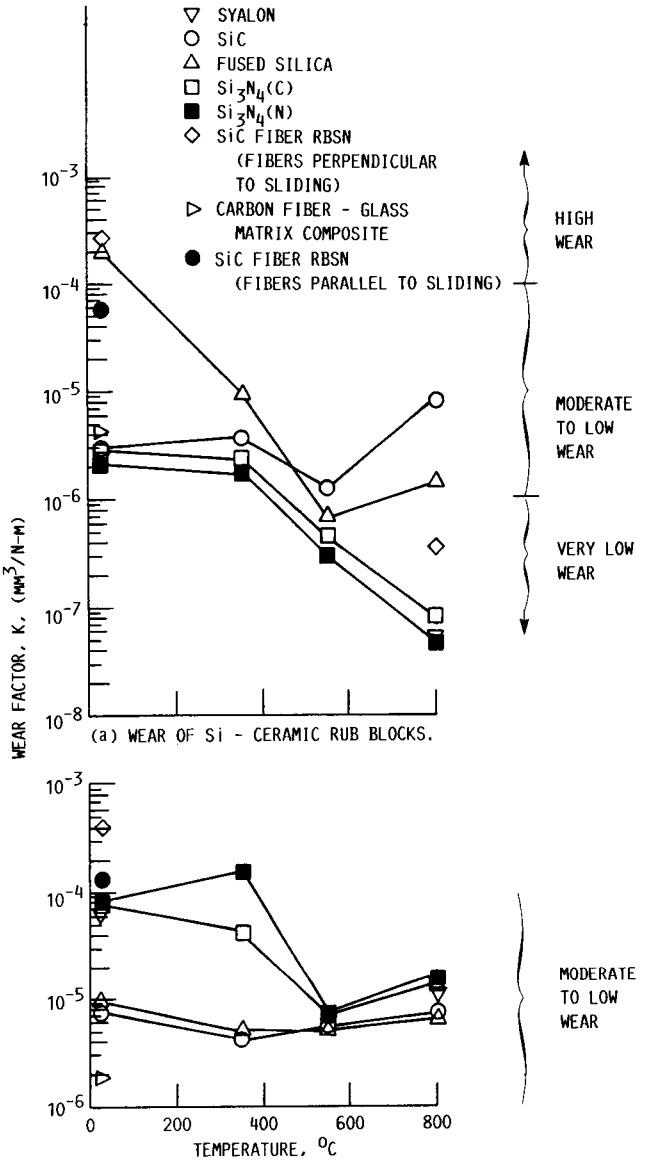

FIGURE 12. - Si - CERAMIC AND IN-718 WEAR VERSUS TEMPERATURE.

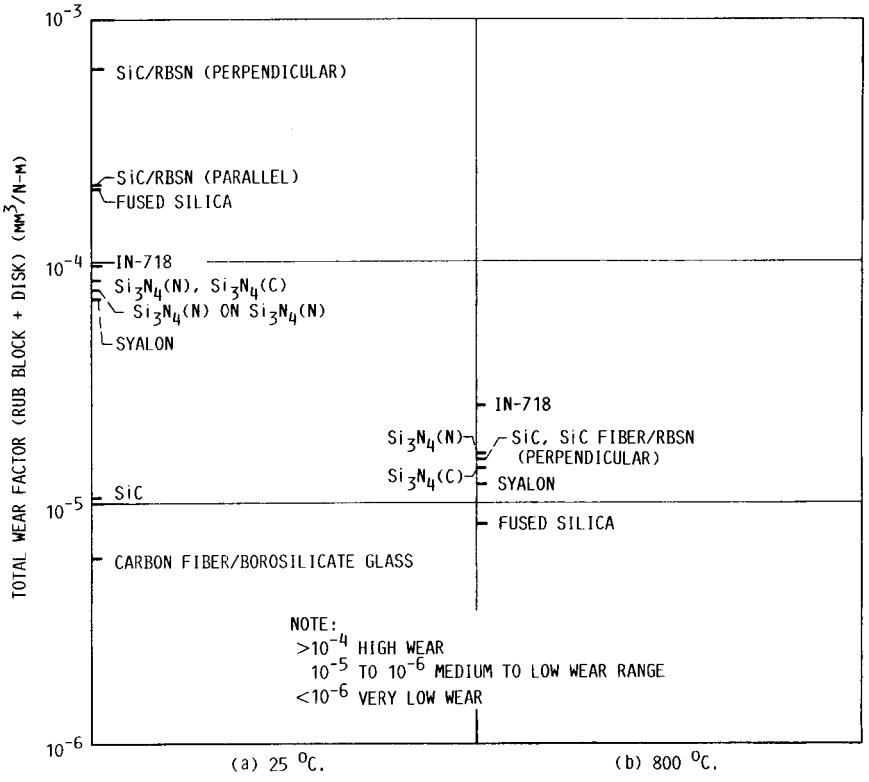

FIGURE 13. - TOTAL WEAR FACTORS OF RUB BLOCKS + DISK AT 25 AND 800 °C. DISK IS IN-718 UNLESS NOTED OTHERWISE.

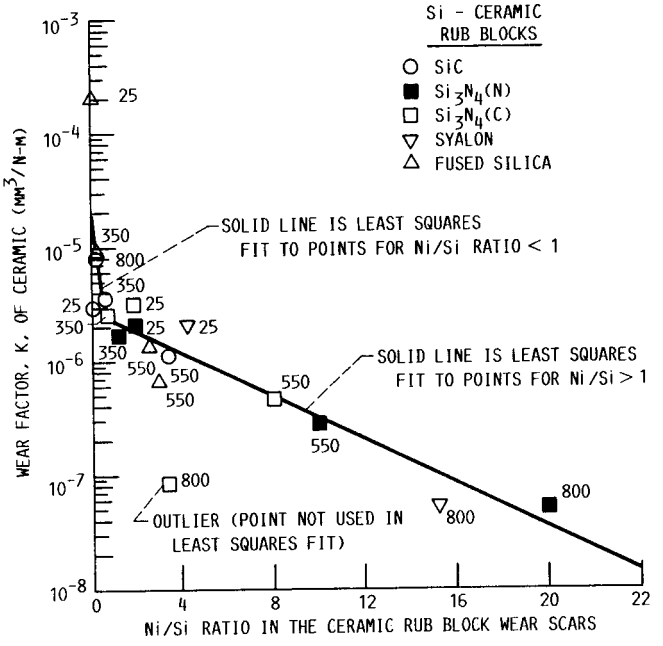

FIGURE 14. - IN-718 ALLOY ELEMENT TRANSFER TO THE Si - CERAMIC VERSUS THE WEAR FACTOR OF THE Si - CERAMIC RUB BLOCKS AFTER SLIDING 1800 M AT 6.8 Kg LOAD IN AIR AT 45-60 PERCENT RH AT 25-800 °C (648 M FOR SiC). NUMBERS NEAR THE POINTS ARE TEST TEMPERATURES, °C.

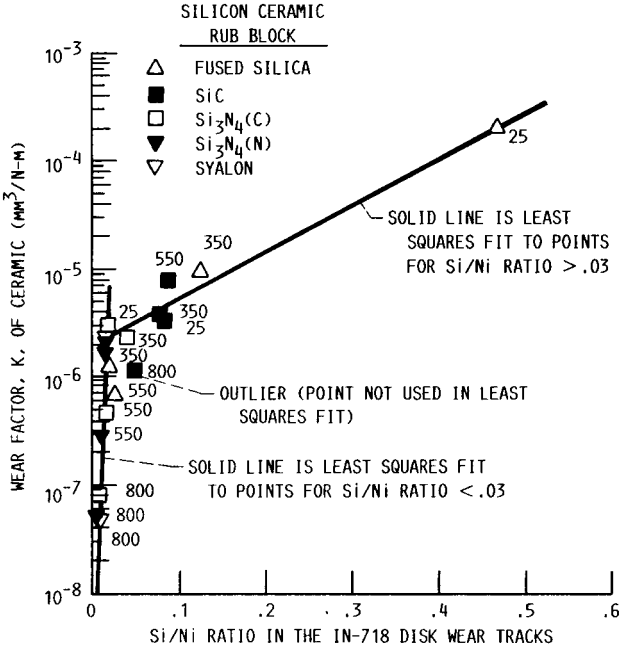

FIGURE 15. - Si - CERAMIC TRANSFER TO THE IN-781 ALLOY DISK VERSUS WEAR FACTOR OF THE Si - CERAMIC RUB BLOCKS - AFTER SLIDING 1800 M AT 6.8 Kg LOAD IN AIR AT 45-60 PERCENT R.H. AT 25-800 °C (648 M FOR SiC). NUMBERS NEAR POINTS ARE TEST TEMPERATURES °C.

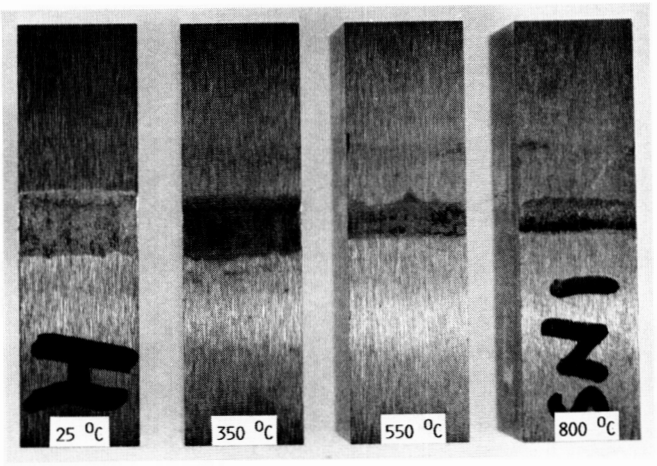

FIGURE 16. - PHOTOGRAPH OF Si_3N_4(N) RUB BLOCKS AFTER SLIDING TEST.

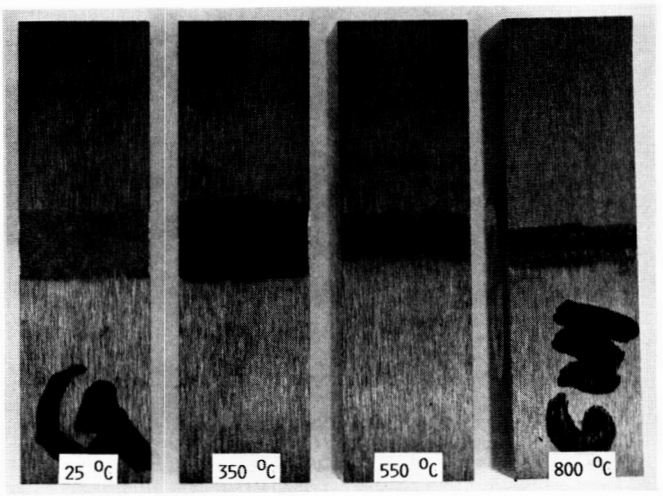

FIGURE 17. - PHOTOGRAPH OF Si_3N_4(C) RUB BLOCKS AFTER SLIDING TESTS.

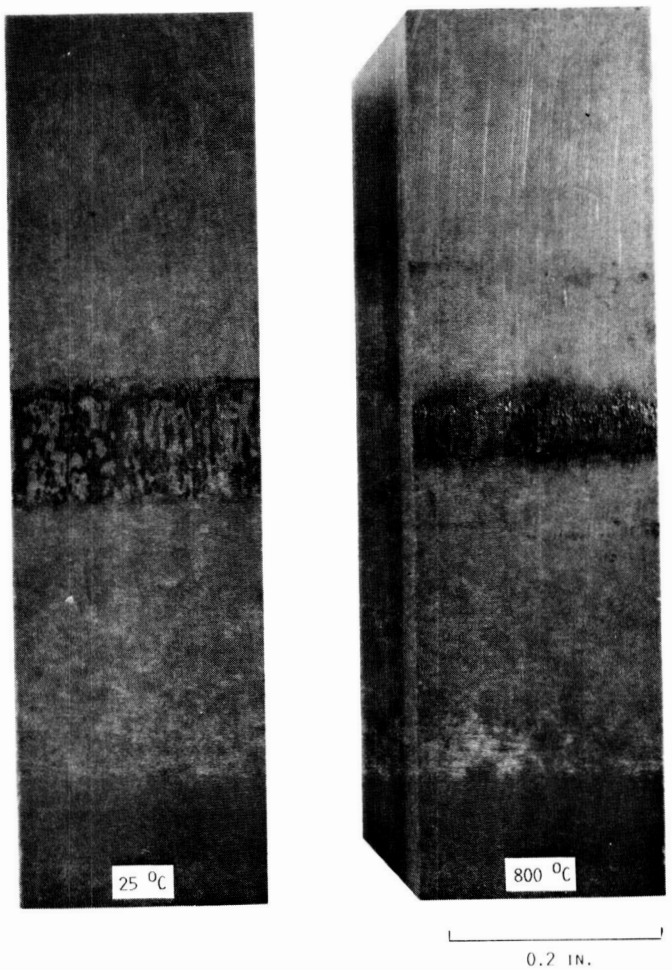

FIGURE 18. - PHOTOGRAPH OF SYALON RUB BLOCKS AFTER SLIDING TEST.

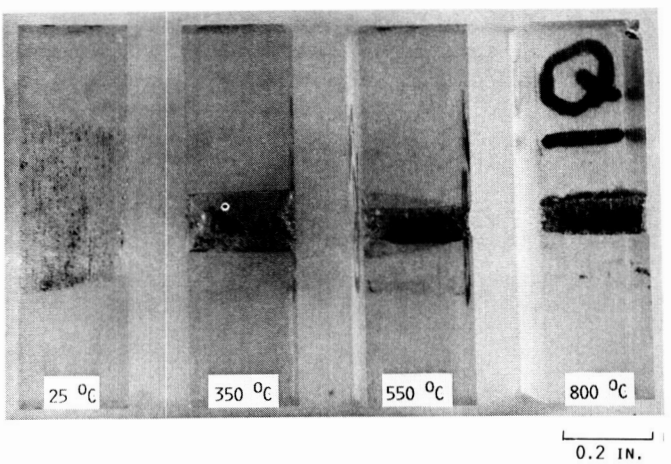

FIGURE 19. - PHOTOGRAPH OF FUSED SILICA RUB BLOCKS AFTER SLIDING TEST.

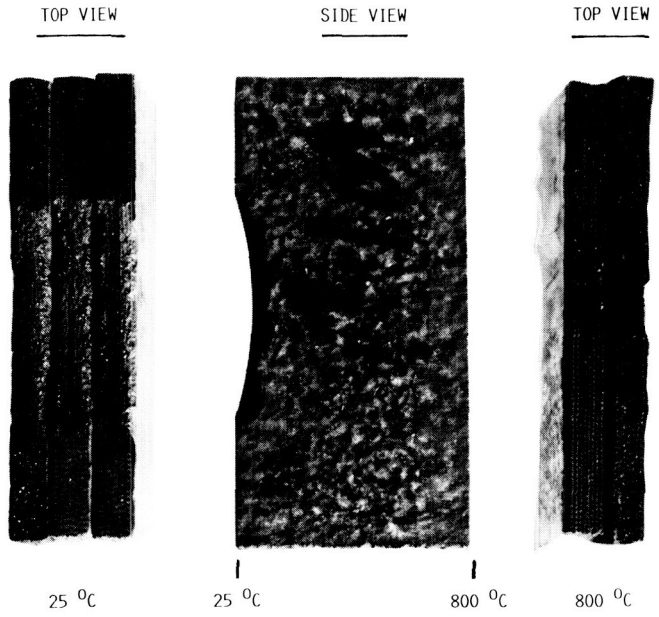

(a) SiC FIBERS PERPENDICULAR TO SLIDING.

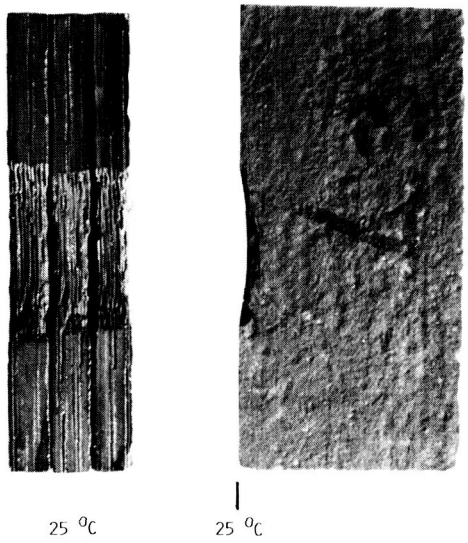

(b) SiC FIBERS PARALLEL TO SLIDING.

FIGURE 20. - PHOTOGRPAH OF SiC FIBER/RBSN RUB BLOCKS AFTER SLIDING TEST AGAINST IN-718 IN AIR AT 25 AND 800 °C.

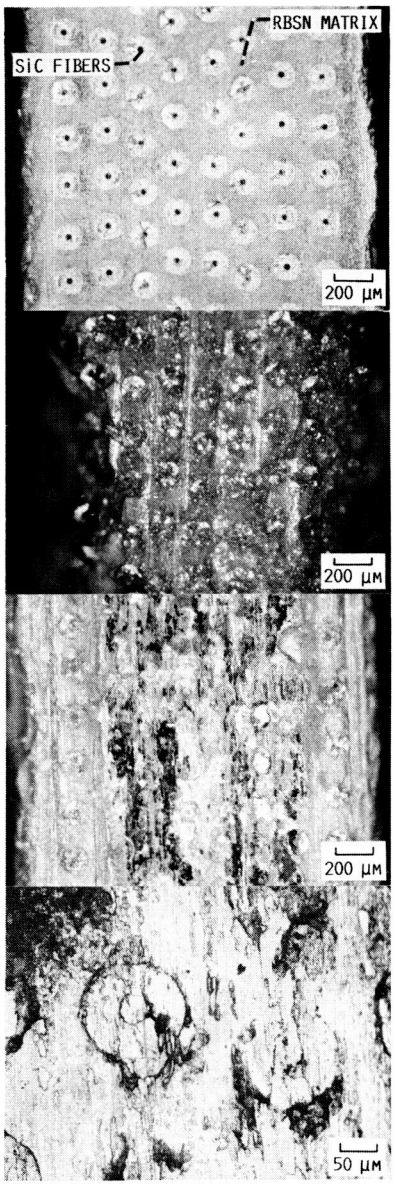

(a) SiC FIBER REINFORCED RBSN - POLISHED ON LEVIGATED Al_2O_3 - BEFORE SLIDING.

(b) WEAR SCAR AFTER SLIDING AT 25 °C FOR 1800 m AT 67N LOAD IN AIR.

(c) WEAR SCAR AFTER SLIDING AT 800 °C FOR 1800 m AT 67N LOAD IN AIR.

(d) WEAR SCAR AFTER SLIDING AT 800 °C FOR 1800 m AT 67N LOAD IN AIR.

FIGURE 21. - PHOTOGRAPHS OF SiC FIBER REINFORCED REACTION - BONDED SILICON NITRIDE MATRIX COMPOSITES BEFORE AND AFTER SLIDING ON IN-718 IN AIR WITH SiC FIBERS PERPENDICULAR TO THE SLIDING SURFACE.

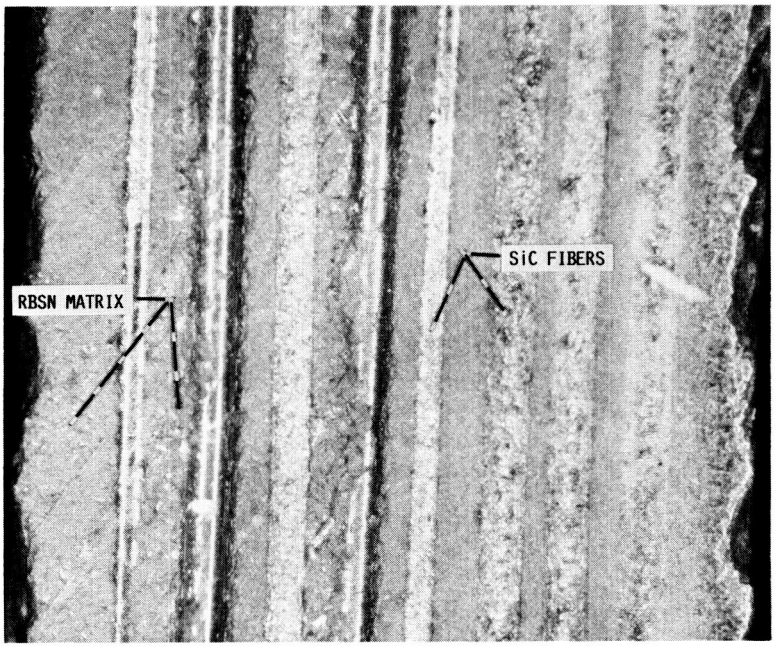

(a) SiC FIBER REINFORCED RBSN BEFORE SLIDING.

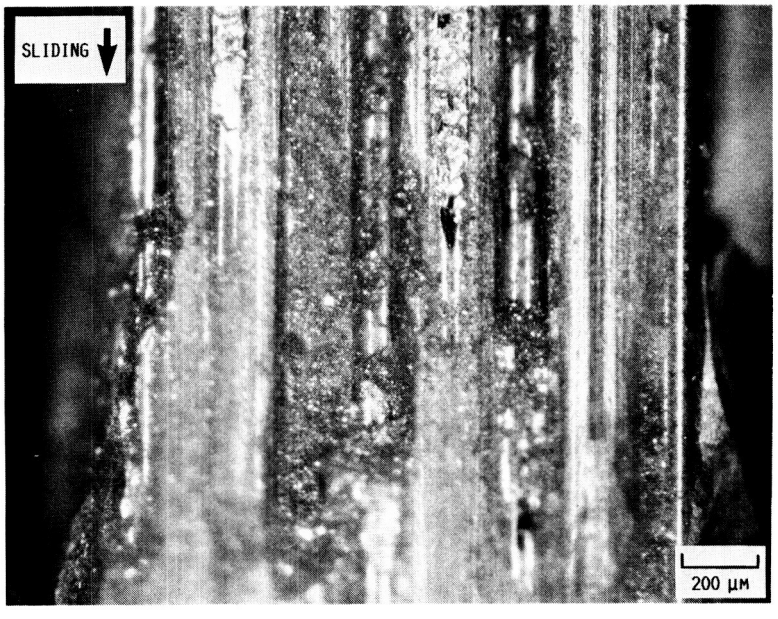

(b) SiC FIBER REINFORCED RBSN WEAR SCAR AFTER SLIDING FOR 1800 m AT 67N LOAD IN AIR AT 25 ^{o}C PARALLEL TO FIBER DIRECTION.

FIGURE 22. - SiC FIBER REINFORCED RBSN COMPOSITE BEFORE AND AFTER SLIDING ON IN-718 ALLOY FOR 1800 m AT 67N LOAD AT 25 ^{o}C IN AIR. SLIDING IS PARALLEL TO FIBER DIRECTION.

NASA
National Aeronautics and Space Administration

Report Documentation Page

1. Report No.	2. Government Accession No.	3. Recipient's Catalog No.
NASA TM-100294		

4. Title and Subtitle
Friction and Wear of Monolithic and Fiber Reinforced Silicon-Ceramics Sliding Against IN-718 Alloy at 25 to 800 °C in Atmospheric Air at Ambient Pressure

5. Report Date
February 1988

6. Performing Organization Code

7. Author(s)
Daniel L. Deadmore and Harold E. Sliney

8. Performing Organization Report No.
E-3942

10. Work Unit No.
505-63-01

9. Performing Organization Name and Address
National Aeronautics and Space Administration
Lewis Research Center
Cleveland, Ohio 44135-3191

11. Contract or Grant No.

13. Type of Report and Period Covered
Technical Memorandum

12. Sponsoring Agency Name and Address
National Aeronautics and Space Administration
Washington, D.C. 20546-0001

14. Sponsoring Agency Code

15. Supplementary Notes

16. Abstract

The friction and wear of monolithic and fiber reinforced Si-ceramics sliding against the nickel base alloy IN-718 at 25 to 800 °C was measured. The monolithic materials tested were silicon carbide (SiC), fused silica (SiO_2), syalon, silicon nitride (Si_3N_4) with W and Mg additives and Si_3N_4 with Y_2O_3 additive. At 25 °C fused silica had the lowest friction while Si_3N_4 (W,Mg type) had the lowest wear (2.2×10^{-6} $mm^3/N-m$). This wear is considered to be in the moderate to low range. At 800 °C syalon had the lowest friction while Si_3N_4 (W,Mg type) and syalon the lowest wear (5×10^{-8} and 5.1×10^{-8} $mm^3/N-m$ respectively). This is considered to be very low wear. The SiC/IN-718 couple had the lowest total wear (ceramic rub block wear + alloy disk wear) at 25 °C. At 800 °C the fused silica/IN-718 couple exhibited the least total wear. SiC fiber reiforced reaction bonded silicon nitride (RBSN) composite material with a porosity of 32 percent and a fiber content of 23 vol % had a lower coefficient of friction and wear when sliding parallel to the fiber direction than in the perpendicular at 25 °C. The coefficient of friction for the carbon fiber reinforced borosilicate composite was 0.18 at 25 °C. This is the lowest of all the couples tested. Wear of this material was about two decades smaller than that of the monolithic fused silica. This illustrates the large improvement in tribological properties which can be achieved in ceramic materials by fiber reinforcement. The reason for this large improvement is the increased fracture toughness produced by the fibers. At higher temperatures (550 to 800 °C) the oxidation products formed on the IN-718 alloy are transferred to the ceramic by sliding action and forms a thin, solid lubricant layer which decreases friction and wear for both the monolithic and fiber reinforced composites.

17. Key Words (Suggested by Author(s))	18. Distribution Statement
Ceramics; Wear; Friction; Metals; Fiber reinforced	Unclassified - Unlimited Subject Category 27

19. Security Classif. (of this report)	20. Security Classif. (of this page)	21. No of pages	22. Price*
Unclassified	Unclassified	30	A03

*For sale by the National Technical Information Service, Springfield, Virginia 22161